# MODELING STEADY-STATE THERMAL DEFECTOSCOPY OF STEEL SOLIDS USING TWO SIDE TESTING

by

***Boban R. ANDJELKOVIĆ**, Biljana R. DJORDJEVIĆ, Miloš D. MILOVANČEVIĆ, and Nataša R. JOVANOVIĆ***

Faculty of Mechanical Engineering, University of Nis, Nis, Serbia

Original scientific paper
DOI: 10.2298/TSCI16S5333A

*In this paper, performing the thermal defectoscopy of a steel solid body by applying the thermovision camera, finite element method and method of filtering experimental data is proposed and implemented. Defect thickness, depth and size are analysed by defined temperature reference levels and simplified methodology. The thermal image processing is based on the proposed method. The applicability of this method can be confirmed by comparing analysis of obtained results with already known methods. The conducted experiment indicates that contactless method is efficient in the defects detection of thin non-complex prismatic parts.*

Key words: *thermal defectoscopy, thermovision image, defect detection, non-destructive testing*

## Introduction

The product control is a significant phase of the serial production. The human visual control, which is represented in the greater part of industry, presents the roughest form of elimination of defected produced pieces. The need for creating new and more precise forms of control and safety of products, considering the development of science and technology, has evolved and the demands for accuracy have increased. In the last few decades, the method of non-destructive testing has stood out as the primary method of examination and testing of defects in materials [1-5].

The thermovision methods are contactless measuring methods and, as such, they have become the basic, necessary methods for controlling most of the production and exploitation phases. They enable the detection of defects in a material on a wide surface in a very short period of time. This type of testing has become a standard during the testing in high-tech systems, aerospace and aeronautics. The requirement to use the thermovision methods is the existence of a specific thermal difference between the object which is being tested and its environment. The thermovision methods are defined as passive or active, depending on the existence of an additional source of infrared radiation.

Passive methods enable the recording of the material surfaces and structures, whose temperatures are significantly different from those of the environment and that, do not require an additional source of infrared radiation [6]. The applications of the passive methods are multiple; the most important areas where they can be applied are: control of industrial pro-

* Corresponding author; e-mail: bandjel@masfak.ni.ac.rs

cesses [7], maintenance of machines and equipment, traffic monitoring, detection of forest fires [8], applications in medicine, biology and agriculture, detection of gases and non-destructive testing of electronic printed circuit boards, *etc.*

Active methods of the thermovision examining require the use of additional sources of infrared radiation in order to achieve a specific thermal contrast. Based on the knowledge of the parameters of the outer impulse, the quantitative estimation of the temperature of the tested object is accomplished [9]. In [10], the implementation of a measurement system for thermovision examining of solar cells and modules during the period of their exploitation is shown, which is included in the methods of active thermovision. One method for examining defects in a solid made of glass is described in [11].

## Known solutions

In the 1980s, Vavilov and Taylor [1] took into consideration the non-destructive thermal methods (TNDT) for material testing and pointed out their ability to provide quantitative information about the hidden defects in the material. There are several significant thermal and spectral features of the materials which need to be considered during the testing of the compactness of their structure and the detection of a possible defect. If a solid material has a defect in its structure in the form of a cavity, delamination, disbond or damage of any shape, the density of the material changes at that very place. The density change affects the process of thermal transmission and thermal conductivity of the material. These changes cause surface discontinuity, which is possible to record with a thermovision camera. The functional dependence of the specified values is described by eq. (1):

$$\alpha = \frac{k}{\rho c_p} \tag{1}$$

Thermal effusivity is the parameter that represents the characteristics of the material and it can be calculated with eq. (2):

$$e = \sqrt{k \rho c_p} \tag{2}$$

The materials of the lower thermal resistance value will heat up more and have higher temperatures, compared to the materials with higher thermal resistance values. The thermal difference is defined with eq. (3):

$$\Delta T = \frac{Q}{\sqrt{e \pi t}} \tag{3}$$

The inner and outer defects of the material are capable of easily transmitting heat because of the lower thermal resistance values. By heating, a higher thermal difference compared to the environment can be achieved in these areas. The result of that effect is that defects on the thermovision image will be warmer surfaces.

## Theoretical basis

The transient temperature distribution $T(x, y, z, t)$ throughout the domain is obtained by solving the 3-D heat conduction equation in the substrate along with appropriate initial and boundary conditions. For a function $T(x, y, z, t)$ of three spatial variables $(x, y, z)$, and the time variable $t$, the heat equation is (4):

$$\rho c_p \frac{\partial T}{\partial t} = \frac{\partial}{\partial x}\left(k\frac{\partial T}{\partial x}\right) + \frac{\partial}{\partial y}\left(k\frac{\partial T}{\partial y}\right) + \frac{\partial}{\partial z}\left(k\frac{\partial T}{\partial z}\right) + Q \qquad \text{or} \qquad \rho c_p \frac{\partial T}{\partial t} - \nabla(k\nabla T) = Q \tag{4}$$

All material properties are considered temperature dependent. Problem can be described like eq. (5):

$$\frac{\partial T}{\partial t} - \alpha\left(\frac{\partial^2 T}{\partial x^2} + \frac{\partial^2 T}{\partial y^2} + \frac{\partial^2 T}{\partial z^2}\right) = 0 \qquad \text{or} \qquad \frac{\partial T}{\partial t} - \alpha\nabla^2 T = 0 \tag{5}$$

For precise determination of a temperature field it is necessary to have all thermal characteristics of the material and boundary conditions, thermal characteristics of the environment and its' influence on the defect detection process. For temperature field recording a thermal imaging camera – IR camera is most frequently used.

A thermal imaging camera is a non-contact measurement device which is able to detect the intensity of radiation in the infrared part of the electromagnetic spectrum and converts it to a thermal crisp real-time high-resolution picture. From these images, temperatures can be read on a screen in real time, and can likewise be sent to a digital storage device for further analysis [12-14]. Infrared radiation (IR) is located between the visible light and microwaves of the electromagnetic spectrum within the wavelength, $\lambda$, of 0.7-1000 μm. Only IR wavelengths between 0.7 μm and 20 μm are used for practical, everyday temperature measurement [15]. The human eye cannot see IR radiation, so the thermal imaging camera acquires IR radiation and transform it into a visible image of radiation emitted from objects because of their temperature and nature of the surface materials [16]. The result is a false – color image, called a thermogram. Thermogram is thermal map of surface where the distribution of thermal energy is represented with different colors [17]. Thermal energy represents total IR energy, which can be reflected, refracted, absorbed and emitted.

The intensity of emitted radiation by an object is a function of its temperature, wavelength, and emissivity. Thermal energy does not radiate similarly for all objects and materials. Emissivity of the surface materials is a term describing its effectiveness in emitting energy as thermal radiation [18]. A perfect emitter, also known as a blackbody, has an emissivity of 1 and radiates the maximum thermal energy possible at each wavelength. The surface of an object whose emissivity is absolute zero (–273.16 °C) emits no IR radiation. Most objects and materials that are used in practical applications, which have constant emissivity values between 0 and 1, are called grey bodies. The lower emissivity of most materials studied in practical applications reduced the intensity of radiation from the theoretical predictions of Planck's Law. This law describes the relationship between spectral emissivity, temperature and radiant energy from a black body. The radiation caused by the temperature T of an object is described by Planck's wavelength distribution function eq. (6):

$$E_{BB}(\lambda, T) = \frac{2hc^2}{\lambda^5}\frac{1}{e^{\frac{hc}{\lambda k_B T}} - 1} \tag{6}$$

Wien's displacement law is obtained by differentiating the Planck's law, eq. (6), with respect to $\lambda$, at which the peak occurs for a specified temperature eq. (7):

$$\lambda_{\max} T = 2898 \tag{7}$$

The relationship between total energy radiation intensity (all wavelengths) and temperature is defined by the Stefan-Boltzmann law (8):

$$E_{BB} = \sigma T^4 \tag{8}$$

When radiation contacts a surface a portion of the energy received will be absorbed ($A$), a portion will be reflected ($R$) and the remaining part, if any, is transmitted ($T$), as illustrated in fig. 1. The fraction of radiation absorbed by the surface is called the absorptivity, the fraction reflected by the surface is called the reflectivity, and the fraction transmitted is called the transmissivity [19]. The total sum of the three individual parts must always add up to the initial value of radiation which left the source.

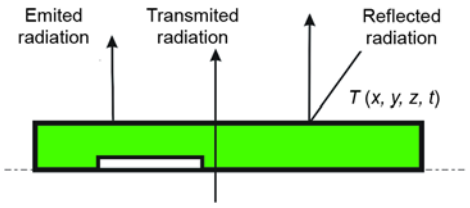


**Figure 1. The reflection and transmission of incident radiation by a target surface**

These three types of energy have a very important role in thermal analysis. The thermal equipment detects all types of energy, but not all indicate the true temperature of the object. These energy types produce three of the four apparent sources of temperature difference (emitted radiation, reflected radiation, transmitted radiation). Reflected radiation is relating to the variations in shape of the target object, its surface texture, and if there are natural cavities created due to the shape of the object. Temperature differences must be taken into consideration so that accurate measurement and comparison of emitted radiation is determined [16].

## Thermal properties – conductivity and effusivity

Thermal diffusivity is defined as the ratio between the thermal conductivity, $k$, and the volumetric thermal capacity, $\rho c_p$, the effusivity, $e$, is related to their product, as in eqs. (1) and (2). Those two expressions contain the same parameters, but diffusivity and effusivity are very different. Diffusivity is related to the speed at which thermal equilibrium can be reached. Effusivity (or the heat penetration coefficient), is the rate at which a material can absorb heat. It is the property that determines the contact temperature of two bodies. The thermal diffusivity is related to time-dependent heat transfer. The contact temperature is time-invariant as long as the two materials may be considered infinite. The controlling parameter of many industrial applications is often effusivity, not the diffusivity.

According to Fourier's law eq. (9):

$$q = \frac{k\Delta T}{\delta} \tag{9}$$

in a controlled environment known variables are the temperature value of heating $T_{\text{con}}$, heat flux $q_{\text{con}}$, and the thickness of experimental specimen, $\delta_{\text{spec}}$, meaning $q_{\text{con}} = k\Delta T_{\text{con}}/\delta_{\text{spec}}$.

Thermal conductivity, $k$, can determined as eq. (10):

$$k = q_{\text{con}} \frac{\delta_{\text{spec}}}{\Delta T_{\text{con}}} \tag{10}$$

Therefore it is possible to determine the thickness of the solid steel body based on the temperature field of the upper side of the solid steel body, eq. (11). This temperature field, however, is a result of IR camera recordings.

$$\delta = \delta_{\text{spec}} \frac{\Delta T \, q_{\text{con}}}{\Delta T_{\text{con}} \, q} \tag{11}$$

Reduction of thickness shows a manifestation of defects in the material. If the calibration phase is skipped, the resulted values of $\Delta T$ and $\delta$ in a metric system based on this principle will be inaccurate, but defect locations will be easily observed presented as deviations of equivalent thickness.

## Simulation analysis

In the interior of the solid steel body, unknown objects and impurities can be detected. Also the discontinuity of the material density can be spotted as a result of disturbance of the production process. The external defects come in the form of physical damage of various shapes.

For a steady state analysis solid steel body with a centered hole shaped defect is used. Analysis shows that the inspected influence of a varying intensity heat flux and different thickness values between the defect location and the upper side to the possibility of locating defect presence in the material. The material of the specimen is plain carbon steel with following properties: elastic modulus $E$ = 2.1e11 N/mm$^2$, Poisson's ratio $\mu$ = 0.28, mass density $\rho$ = 7800 kg/m$^3$, and thermal conductivity $k$ = 55 W/mK.

Geometric model finite element analysis is created as solid body that consists of 3-D tetrahedral finite elements. The global geometry has been simplified by removing less important areas. The DC3-D4 a 4-node linear heat transfer tetrahedron element is used for a steady state analyses, simplified model is shown in fig. 2.

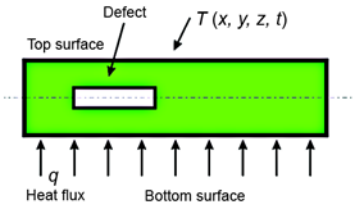


**Figure 2. Simplified model for finite element analysis**

After completion of the finite element model, it was necessary to apply constraints, loads and interactions to the model. The steady state analyzed specimen was subjected to the constant heat flux from the bottom side of the solid steel body (fig. 2). Environmental interaction is defined as the radiation of all other surfaces, except bottom side, in a 20 °C temperature span.

This type of static simulation is used for its' simplicity and simple required equipment operation. Other forms of measure, for example a dynamic, would require equipment more expensive and complicated equipment.

Results of finite element model analysis are temperature fields presented in figs. 3-10. Temperature fields are determined for different values of heat flux and material thickness above the hole shaped defect. Temperature field in a longitudinal and transverse direction is presented on figs. 9 and 10. For cases with deeply imbedded defects, confirming defect presence by using the temperature field is impossible. Temperature decrease or a deviation of equivalent thickness has low value and thus might be misinterpreted as disturbance instead of a defect presence (fig. 7). Increasing the heat flux value does not contribute to result readability. These cases require inspection based on a varying heat flux that also requires more complicated equipment.

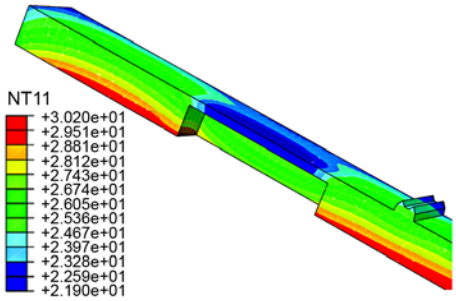


**Figure 3. $q$ = 50 W/m$^2$, $\delta$ = 5 mm**
*(for color image see journal web-site)*

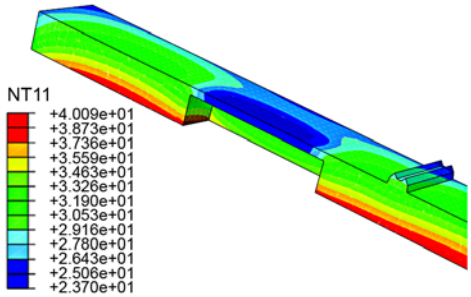


**Figure 4. $q$ = 100 W/m$^2$, $\delta$ = 5 mm**
*(for color image see journal web-site)*

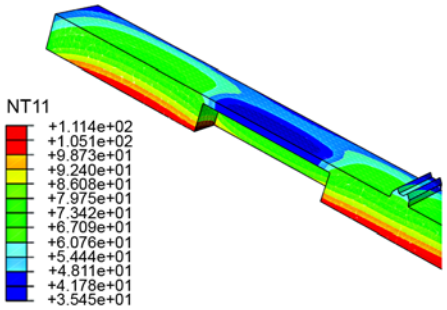


**Figure 5. $q$ = 500 W/m$^2$, $\delta$ = 5 mm**
*(for color image see journal web-site)*

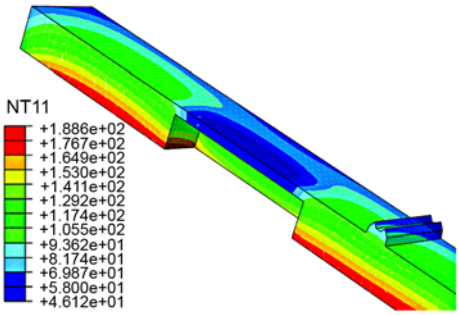


**Figure 6. $q$ = 1000 W/m$^2$, $\delta$ = 5 mm**
*(for color image see journal web-site)*

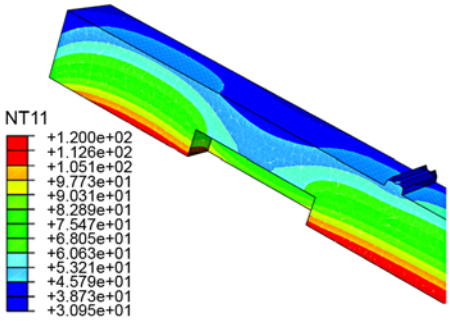


**Figure 7. $q$ = 500 W/m$^2$, $\delta$ = 10 mm**
*(for color image see journal web-site)*

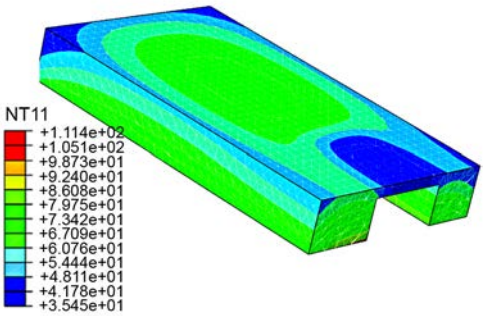


**Figure 8. Transversal cross section**
*(for color image see journal web-site)*

## Experiment

The goal of the research is to confirm the possibility of applying non-destructive methods of examining and detecting material defects of thin non-complex prismatic parts. The

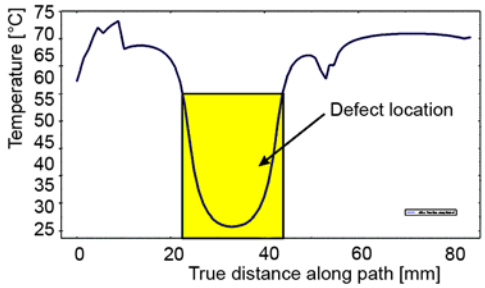


**Figure 9. Temperature deviation in longitudinal direction**

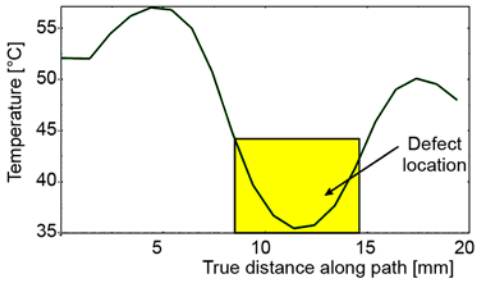


**Figure 10. Temperature deviation in transverse direction**

conducted experiment employs a thermovision system in combination with a personal computer. The material of the used samples is steel. Such a manner of testing allows for the detection of defects in the material on a big surface and in a relatively short period of time. The system is designed in order to perform the process of product control without human presence. The used samples (fig. 11) are rectangular in shape. The samples were degreased and coated with protective paint so that the emissivity is spread uniformly over the entire surface. This is a simple procedure and allows an accurate analysis of the issue at hand.

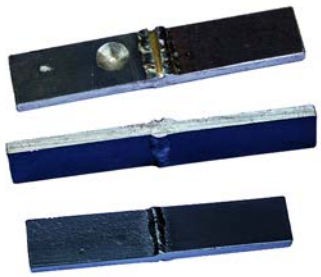

**Figure 11. Specimen for IR analysis**

The applied method belongs to the group of active methods because it requires an additional source of energy in order to achieve the needed thermal difference between the object and its environment. The constant thermal flux is used for that purpose. It provides the needed amount of heat for the samples, and thus enables thermovision camera recording. The constant thermal flux is positioned below the specimen (fig. 12).

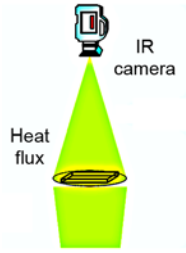


**Figure 12. Disposition of measuring equipment**

Once the object is recorded, the signal is transmitted from the thermovision camera to the computer where it gets adequately transformed. The transformed signal is then being processed by means of appropriate software and a thermogram is formed. The obtained results can be displayed on the screen in the form of a 3-D presentation or a 2-D diagram. With the aim of detecting possible defects in the material, first the recording of the reference sample without defects is performed in the state of inaction. The analysis of the reference model thermogram yields the values of temperature dilatations which are caused by surface roughness. By recording the unexamined object, forming its thermogram and analyzing it in comparison to the previously obtained thermograms of the reference model, one can observe the existence of a defect in the material.

The heat that is emitted by the object after its passing through the atmosphere and camera lens reaches the detector. The detector transforms the received signal into an electrical signal and sends it to the computer system. The same signal is shown on the screen as a colorful image – thermogram. The camera registers the simultaneous radiation off of the object sur-

face as well as the atmospheric radiation. Since only the energy emitted by the object itself is important for the research, it is necessary to compensate for the influence of the atmospheric radiation. This compensation is achieved with the help of the correctional parameters that include distance between the object and the camera, relative environment humidity and environment temperature. In order to minimize the atmospheric effects, the experiment is carried out in the laboratory conditions.

The difference and discontinuity in the model of the examined sample is observed when it is compared to the reference model thermogram. It is assumed that the structure of sample, thin, non-complex prismatic parts is homogeneous. For the thermogram analysis software package MATLAB was used. The filtering process is carried out in the direction of the x-axis, y-axis as well as in both directions simultaneously. Low result values of the test model indicate the structure is homogeneous. With the analysis of obtained results the maximal value has been determined and taken as a reference parameter. The reference sample as well as the test sample is exposed to the same environmental conditions. The existence of defects is deducted from the comparison of obtained results with referent parameters (figs. 13-16).

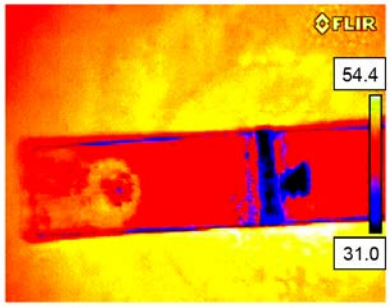


**Figure 13. Thermal image of heated sample**
*(for color image see journal web-site)*

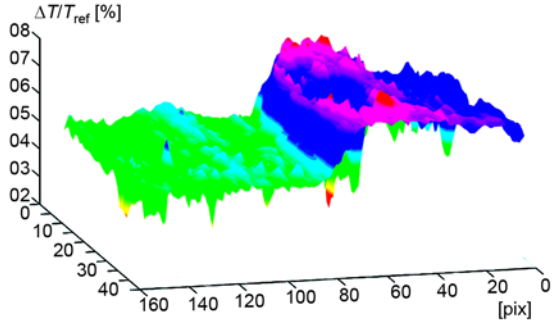


**Figure 14. The IR thermogram of sample with defect**
*(for color image see journal web-site)*

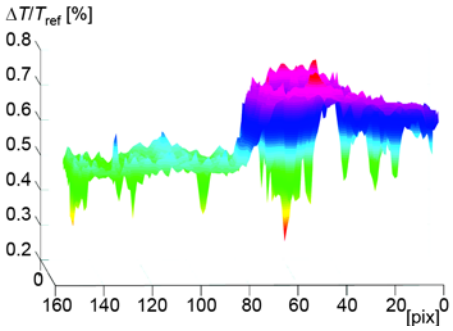


**Figure 15. Position of defect – x-axis**
*(for color image see journal web-site)*

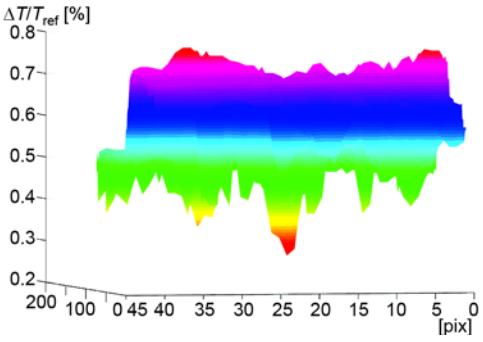


**Figure 16. Position of defect – y-axis**
*(for color image see journal web-site)*

Filtering is performed in two mutually perpendicular directions. The obtained results show the presence or absence of defects. A defect can be detected if its shape and direction of distribution are at a random angle or match the direction of the filter kernel movement. If the defect is in the direction perpendicular to the direction of the filter kernel movement, there is no possibility for it to be detected. With the aim of solving this problem, filtering is conducted

in both directions simultaneously. This enables the detection of defects regardless of their shape and position.

For the estimation of the parameters of the reference model the filtering in two perpendicular directions is conducted. Figure 17 presents 3-D example of the referent sample thermal dilatation. A relatively even distribution is noted, due to its homogeneous structure and the deviations are the result of the surface roughness. A reliable detection of defects, regardless of their shape and size, can be realized by using the simultaneous filtering in two perpendicular directions. The most reliable results are obtained by applying the filtering kernel with dimensions (3 pix. × 3 pix.).

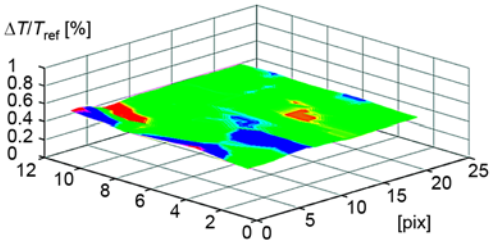


**Figure 17. Reference model – sample without any defect** *(for color image see journal web-site)*

The change in the numerical values of the 2-D filtering results is in the dependence of the current filtering kernel position. This change is the result of surface roughness of the reference sample. The criterion in the process of defect detection is the maximal value of thermal deviation. This value is considered to be the threshold value. By analyzing the thermogram of the untested object and comparing its parameters with the approved threshold value, the data about the existence of defects on the object can be obtained. If thermal deviations are greater than the threshold value in some points that implicates that the distribution of the heat in those points are significantly increased. Discontinuity of the thermal distribution is the direct result of the existence of defects. Figure 13 shows a sample with the defect. The heat distribution is presented in figs. 14-16. A significant deviation can be seen in certain domain, which is the result of the defect in the structure.

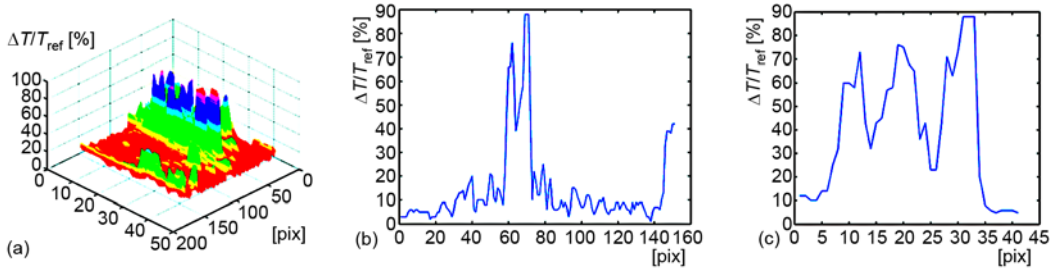


**Figure 18. The 2-D filtering of the thermogram of a sample** *(for color image see journal web-site)*

The defects in both directions are detected by 2-D filtering of the thermogram in x-y plane. A comparison of the obtained results with the reference values is enabled by applying the same filtering kernel which was used for the filtering of the reference model. The results of the analysis indicate the existence of defects. The 3-D presentation of the obtained results is shown in fig. 18(a). The distribution of the thermal changes in x-z plane is presented in fig. 18(b), and the distribution of these changes in y-z plane is presented in fig. 18(c). The position of the largest detected defect on the tested object is determined by using appropriate algorithms.

## The system proposed for practical use

The suggested system consists of test sample, thermovision camera and computing system for the data processing. The sample is affected by evenly distributed surface thermal

flux. Heat source as well as thermovision camera are positioned on the opposite sides of the sample. After the recording, the signal is led from the thermovision camera to the computing system, transformed, and then presented on screen. The analysis of the thermogram is carried out by applying the software package, which consists of five sequential processes. First process is to upload and pre-processing image of the heated sample without defects. Then filtering process in two perpendicular directions and analysis of the filtering results with estimation of the allowed thermal dilatation value is done. After uploading image of the defected object, filtering is carried out in both directions simultaneously. Result of heated sample without defects and defected object are compared.

## Conclusions

The presented principle of thermography, the procedure for testing, and the obtained results indicates that method of indirect testing is very useful when it comes to assessing and discovering defects with the possibility of monitoring the development of defects. Determination of the defects, existence and the location in products after a certain exploitation period is the subject of numerus experimental research. The presence of defects causes undesirable changes in product features. Defects most often occur during the production or exploitation processes. The implemented system presents an original solution that increases the possibilities of a steady-state testing and product quality control in exploitation. Presented research results imply possibility in increase in efficiency and expand the basic application of the thermovision system. The research presented in this paper, is foundation for the contactless determination of defects or the presence of thin non-complex prismatic objects in the structure of a product.

The measuring system consists of a heat source at the bottom and infra-red camera at the top of the tested specimen. System can be used in production lines for detecting defects in material rolling mill. It is optimal for exploitation in industrial conditions since the lower accuracy isn't suitable for laboratory applications. The measuring system is able to detect the cavities, delamination and variation of material density that are located in vicinage of top surface. For defects located deep in the material, it is impossible to determine their existence with certainty. Therefore, application of these a steady state method is recommended for of thin non-complex prismatic objects, as sheets in rolling mills. In many cases, the standards allow the presence of cavities or defects of certain dimensions and frequency.

The results demonstrated that the proposed method has exploitation potential, especially in rolling mill industry, although further refinements are needed in order to apply the method industry.

## Nomenclature

$c$ – velocity of light (= $3\cdot10^{8}$), [ms$^{-1}$]
$c_p$ – specific heat capacity, [Jkg$^{-1}$K$^{-1}$]
$E_{BB}$ – spectral radiant emittance, [Wm$^{-2}$μm$^{-1}$]
$e$ – effusivity, [Ws$^{1/2}$m$^{-2}$K$^{-1}$]
$h$ – Planck's constant (= $6{,}625\cdot10^{-34}$), [Js]
$k$ – thermal conductivity, [Wm$^{-1}$K$^{-1}$]
$k_B$ – Boltzmann's constant (= $1{,}38\cdot10^{-23}$), [JK$^{-1}$]
$Q$ – heat source or sink, [J]
$\Delta T$ – temperature increase or decrease, [K]
$T$ – temperature, [K]
$t$ – time, [s]

*Greek symbols*

$\alpha$ – thermal diffusivity, [m$^2$s$^{-1}$]
$\delta$ – thickness, [mm]
$\lambda$ – wavelength, [μm]
$\rho$ – density, [kgm$^{-3}$]
$\sigma$ – Stefan-Boltzmann constant ($5{,}6697\cdot10^{-8}$), [Wm$^{-2}$K$^4$]

## References

[1] Vavilov, V. P., Advances in Signal Inversion with Application to Infrared Thermography, in: *Advances in Signal Processing for Nondestructive Evaluation of Materials* (ed. Maldague, X. P.), Springer, Netherlands, pp. 161-184, 1994
[2] Maldague, X. P. V., *Theory and Practice of Infrared Technology for Nondestructive Testing*, John Willey and Sons Inc., New York, NY., USA, 2001
[3] Heriansyah, R., Abu-Bakar, S. A. R., Defect Detection in Thermal Image using Thresholding Technique, *Proceedings*, 6th WSEAS International Conference on Circuits, Systems, Electronics, Control & Signal Processing, Cairo, Egypt, 2007, pp. 29-31
[4] Corke, P., *Robotics, Vision and Control*, Springer-Verlag Berlin, Heidelberg, Germany, 2011
[5] Petrušić, Z., *et al.*, Active Thermovision Method for Inspection of Solar Cells, *Proceedings*, Infoteh, Jahorina, Bosnia & Herzegovina, Vol. 8 (2009), pp. 449-455
[6] Prijić, A., *et al.*, Design and Optimization of S-Type Thermal Cutoffs, *IEEE Trans. on Components and Packaging Technologies, 31* (2008), 4, pp. 904-912
[7] Rao, M. R. P. D., Review of Nondestructive Evaluation Techniques for FRP Composite Structural Components, M. Sc. thesis, College of Engineering and Mineral Resources at West Virginia University, Morgantown, West Virginia, USA, 2007
[8] Choi, C. J., *et al*., Study on the Application of Infrared Thermovision Camera for Efficiency Analysis of Solar Cell, *Material Science Forum*, Vols. 544-545 (2007), pp. 467-470
[9] Stević, Z., *et al*., Computer Based Infrared Thermography System for Monitoring and Diagnostics in Electroenergetic Plants, *Proceedings*, Infoteh, Jahorina, Bosnia & Herzegovina, Vol. 5 (2009), pp. 225-229
[10] Wierzbicki, L., *et al*., Efficiency of Two Nondestructive Testing Methods to Detect Defects in Polymeric Materials, *Journal of Achievements in Materials and Manufacturing Engineering*, 38 (2010), 2, pp. 163-170
[11] Andjelković, B., *at al.*, Modeling of Defects Detection by Analyzing Thermal Images, *Facta Universitatis, Series: Mechanical Engineering*, *12* (2014), 2, pp. 123-136
[12] Wierzbicki, L., *at al.*, Detecting of Defect in Polymeric Materials Using Pulsed Infrared Thermography, *Archives of Materials Science and Engineering, 30* (2008), 1, pp. 29-32
[13] Rogalski, A., Chrzanowski K., Infrared Devices and Technique (revision) *Metrology and Measurement Systems*, *21* (2014), 4, pp. 565-618
[14] ***, IR Automation Guidebook: Temperature Monitoring and Control with IR Cameras, FLIR Systems Inc., Boston, Mass., USA, 2008
[15] Gade, R., Moeslund, T. B., Thermal Cameras and Applications, A Survey, *Machine Vision & Applications, Denmark, 25* (2014), 1, pp. 245-262
[16] ***, Facilities Instructions, Standards, and Techniques, *Thermal Analysis*, Denver, Colorado, 2011
[17] Gaussorgues, G. *Infrared Thermography*, Springer, Berlin/Heidelberg, Germany, 1994
[18] Abdalrahman, Z. A. *et al.*, Investigation and Present of the Thermal Imaging Camera, *International Journal of Innovative Science, Engineering & Technology, 2* (2015), 2, pp. 198-201
[19] Lienhard, J. H. IV, Lienhard, J. H. V, *A Heat Transfer Textbook – Fundamentals of thermal radiation*, Phlogiston Press, Cambridge, USA, 2008

Paper submitted: March 31, 2016
Paper revised: May 8, 2016
Paper accepted: May 18, 2016